Tuning Carbon Nanotube Band Gaps with Strain

E. D. Minot, Yuval Yaish, Vera Sazonova, Ji-Yong Park, Markus Brink, and Paul L. McEuen

Laboratory of Atomic and Solid-State Physics, Cornell University, Ithaca, New York 14853
(Received 6 November 2002; published 15 April 2003)

We show that the band structure of a carbon nanotube (NT) can be dramatically altered by mechanical strain. We employ an atomic force microscope tip to simultaneously vary the NT strain and to electrostatically gate the tube. We show that strain can open a band gap in a metallic NT and modify the band gap in a semiconducting NT. Theoretical work predicts that band gap changes can range between ± 100 meV per 1% stretch, depending on NT chirality, and our measurements are consistent with this predicted range.

The electronic and mechanical properties of carbon nanotubes (NTs) are remarkable. A NT can be either metallic or semiconducting depending on the orientation between the atomic lattice and the tube axis [1,2]. NTs can accommodate very large mechanical strains [3], have an extremely high Young's modulus [4], and have interesting electromechanical properties [5–13]. A pioneering experiment [10] showed that the conductance of a metallic NT could decrease by orders of magnitude when strained by an atomic force microscope (AFM) tip. The authors suggest that a local distortion of the sp^2 bonding where the NT is touched by the AFM tip causes the drop in conductance. In Ref. [12], however, it is argued that the observed drop in conductance is due to a band gap induced in the NT as it is axially stretched [5,8,11], as illustrated in Fig. 1(a).

Here we present measurements to demonstrate conclusively that strain modulates the band structure of NTs. We employ an AFM tip to simultaneously vary the NT strain and to electrostatically gate the tube. We find that, under strain, the conductance of the NT can increase or decrease, depending on the tube. By using the tip as a gate, we show that this is related to the increase or decrease in the band gap of a NT under strain. The magnitude of the effect and its dependence on strain are consistent with theoretical expectations.

The samples consist of NTs suspended over a trench and clamped at both ends by electrical contacts [10,14–17]. Chemical vapor deposition growth is utilized to grow NTs with diameters between 1 and 10 nm at lithographically defined catalyst sites [18] on a Si substrate with a 500 nm oxide. Metal contacts (5 nm Cr and 50–80 nm gold) are made using photolithography, as described previously [19]. An ashing step (400 °C for 10 min in Ar atmosphere) removes photoresist residue and improves contact resistances. An HF etch (3 min in 6:1 BHF, etch rate 80 nm/min) followed by critical point drying is used to suspend the NTs [16]. Device conductances are not changed significantly by the etching/drying procedure [20].

The suspended tubes are then placed in a commercial AFM system (Dimension 3100, Digital Instruments) for simultaneous electrical measurements and AFM imaging/manipulation [21]. The AFM tips used (Nanosensor EFM tip) have a nominal radius of 20 nm, cantilever spring constants of 1–5 N/m, and are coated with a PtIr metal layer. Spring constants were calibrated using the thermal noise method [22]. To probe the mechanical and electromechanical properties, the AFM tip is centered above a suspended NT using a tapping mode image for guidance. The tip is then moved in the z direction as illustrated in Fig. 1(b), while monitoring the static deflection of the cantilever and/or the conductance of the tube [23].

Plotted in Fig. 2 is the upward force on the cantilever F_z as a function of the tip height z while raising the AFM tip. Figure 2 shows that the force the tube exerts on the tip can be both positive (upward) as well as negative (downward). These are separated by a region of near-zero force when the tip is near the plane of the contacts.
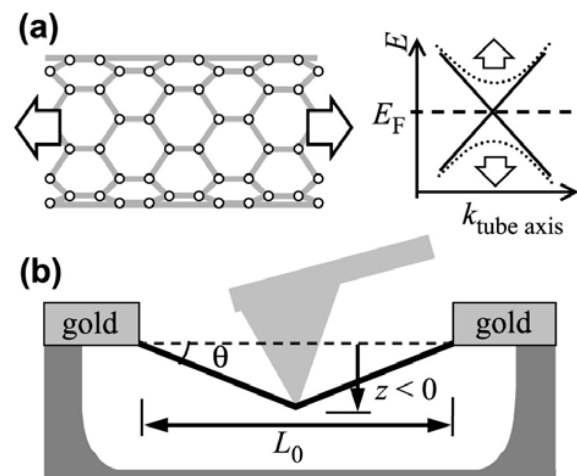

FIG. 1.   (a) Real space representation of a zigzag NT and the dispersion relation near E_F. Solid lines and dashed lines show $E(k)$ before and after stretching, respectively. (b) Experimental geometry for applying strain and gate voltage with an AFM tip, and measuring conductance with gold contacts. L_0 is distance between anchoring points; z is the distance the center of the NT is displaced from the plane of the anchoring points.
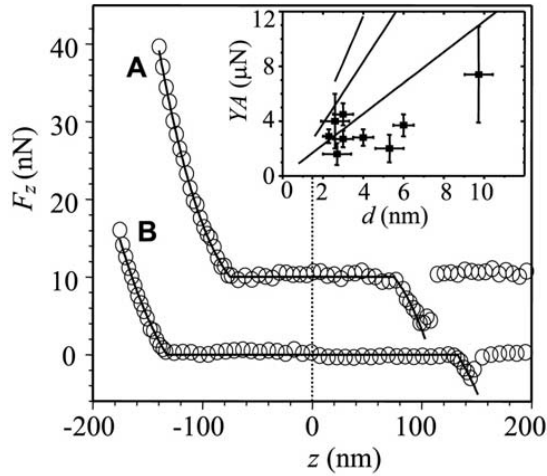
FIG. 2. Force-distance curves of two NTs; curve A is offset for clarity. Open circles show the measured deflection force as the AFM tip retracts towards positive z. Curve A is from a NT with $d = 5.3 \pm 0.5$ nm, $L_0 = 1.0 \pm 0.1$ μm. Curve B is from a NT with $d = 2.3 \pm 0.5$ nm, $L_0 = 1.5 \pm 0.1$ μm. Solid lines are fit curves given by Eq. (1). In curve A, slack = 11 nm, $YA = 2$ μN, and curve B slack = 22 nm and $YA = 2.9$ μN. The tubes were not measured by the same AFM cantilever. The inset shows a summary of fitted YA values. Solid lines are predicted YA for single-, double-, and triple-walled NTs of outer diameter d when all shells carry the same mechanical load [24–26].

Force-distance curves such as Fig. 2 indicate that there is significant adhesion between the AFM tip and the NT. This adhesion has been observed and discussed by other authors [27]. From the distance between pushing and pulling onsets, $\pm z_{\text{onset}}$, the "slack" of a suspended NT can be determined. The slack is defined as $L_{\text{tube}} - L_0$, where L_{tube}, the tube length, is greater than L_0, the separation between the anchoring points. Nearly all NTs measured were slack, with typically 5–10 nm of slack for a 1 μm tube. The slack is consistent with the slightly curved paths NTs followed across the oxide surface before etching.

We find that force-distance curves such as Fig. 2 can be accurately fit by ignoring the bending modulus of the tube and assuming a linear proportionality between NT tension T and axial strain σ. We write the proportionality constant as YA, where Y is an effective Young's modulus, and A is an effective cross-sectional area:

$$F_z(z) = 2T \sin\theta = 2YA\sigma(z)\left(\frac{2z}{\sqrt{L_0^2 + 4z^2}}\right) \quad (1)$$

for $|z| \geq z_{\text{onset}}$ and $F_z(z) = 0$ for $|z| \leq z_{\text{onset}}$

where $\sigma(z) = (\sqrt{L_0^2 + 4z^2} - L_{\text{tube}})/L_{\text{tube}}$ for $|z| \geq z_{\text{onset}}$. A summary of fitted YA parameters is given in the inset of Fig. 2 [28]. The magnitude of YA values and linearity with diameter d suggest that a single shell is carrying the mechanical load, even for large diameter tubes which likely have multiple walls. Similar observations of YA

magnitude [4] and outer-shell loading [3] have been reported.

To probe the electromechanical response of the NTs, we monitor conductance G using a lock-in amplifier and control AFM tip voltage V_{tip}, while straining the tubes. Figure 3 shows both F_z and G, while engaging and then retracting from a NT. V_{tip} is held at 0 V. When the cantilever is deflected, G is lowered, in agreement with previous results [10]. Interestingly, other tubes showed different behavior. Of the seven samples studied, two semiconducting tubes showed *increasing G* when strained, one semiconducting and two metallic tubes showed decreasing G when strained, and two metallic tubes showed no significant change.

To understand the origin of this behavior, the tip is used as a gate to investigate the band structure of the NT under strain. V_{tip} is swept ~3 times a second over a range of a few volts as strain is slowly increased [29]. G vs V_{tip} for different strains are shown in Fig. 4 for two NTs. At no strain ($\sigma = 0$), the observed V_{tip} dependence indicates that the tube of Fig. 4(a) is metallic (G is independent of V_{tip}) and the tube of Fig. 4(b) is semiconducting (G is strongly dependent on V_{tip}). As the metallic tube [Fig. 4(a)] is strained, an asymmetric dip centered at $V_{\text{tip}} \approx 1$ V develops in G-V_{tip}. On the other hand, the semiconducting tube shows an increase of G with strain and a reduction in the asymmetry of the dip. The insets show the maximum resistance $R_{\max}(\sigma)$ for each sweep of V_{tip} as a function of strain, along with a fit to the functional form:

$$R_{\max}(\sigma) = R_0 + R_1 \exp(\beta\sigma). \quad (2)$$

This functional form fits the data well in both cases, but with different values of R_0, R_1, and β.

These results can be understood by the effect of strain on the band gap of the tube, as described by previous
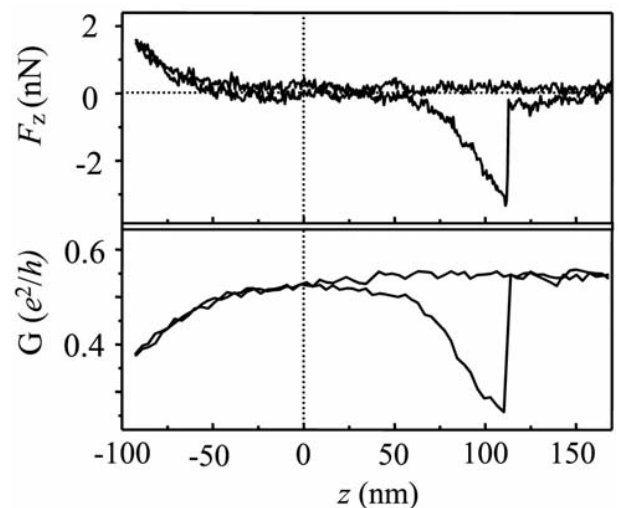

FIG. 3. Deflection force and conductance as a function of tip height for a NT with $d = 6.5$ nm and $L_0 = 1.9$ μm at $V_{\text{tip}} = 0$ V. The tip was first moved toward the surface (toward negative z) and then away from the surface.
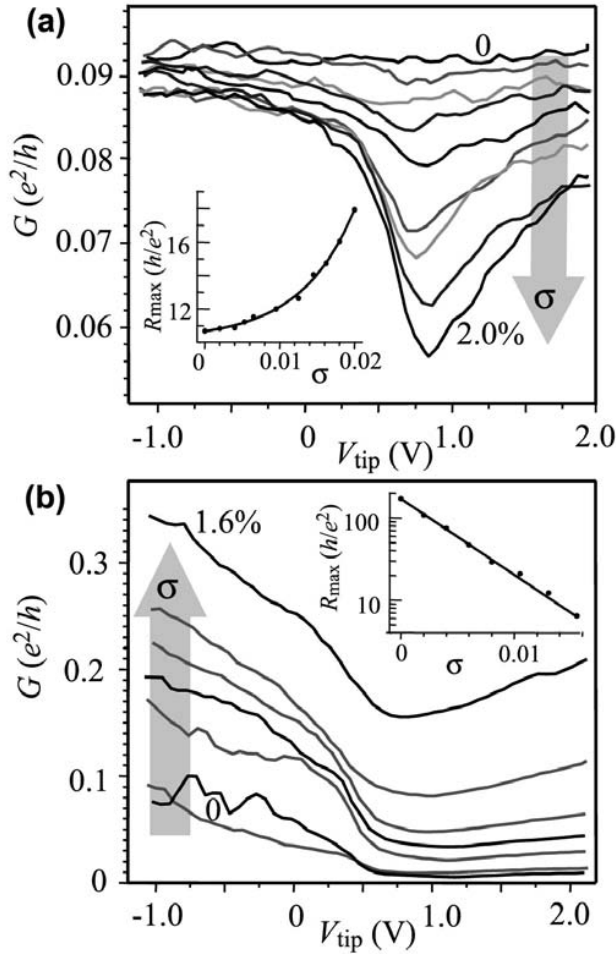
FIG. 4. (a) G-V_{tip} measurements of a NT with $d = 3 \pm 0.5$ nm and $L_0 = 1.4 \pm 0.1$ μm at 0, 0.5, 0.7, 1.0, 1.2, 1.4, 1.6, 1.8, and 2.0% strain. (b) G-V_{tip} measurements of a NT with $d = 4 \pm 0.5$ nm and $L_0 = 1.1 \pm 0.1$ μm at 0, 0.2, 0.6, 0.8, 1.1, 1.3, and 1.6% strain. Closed circles in the insets show maximum device resistance as a function of strain. Solid lines in the insets show fit curves given by Eq. (2). For (a) $R_0 = 10.2h/e^2$, $R_1 = 0.5h/e^2$, and $\beta = 139$. For (b) $R_0 = 0h/e^2$, $R_1 = 171h/e^2$, and $\beta = -213$.

authors [5,8,11]. These papers predict a chirality dependent value for the rate of change of band gap with respect to strain, $dE_{gap}/d\sigma$. From Ref. [11],

$$\frac{dE_{gap}}{d\sigma} = \text{sign}(2p + 1)3t_0(1 + v)\cos 3\phi, \qquad (3)$$

where $t_0 \approx 2.7$ eV is the tight-binding overlap integral, $v \approx 0.2$ is the Poisson ratio, ϕ is NT chiral angle, and $p = -1, 0,$ or 1 such that the wrapping indices, n_1 and n_2, satisfy $n_1 - n_2 = 3q + p$, where q is an integer [11]. The maximum value of $|dE_{gap}/d\sigma|$ is $3t_0(1 + v) \approx 100$ meV/%, similar in magnitude to $|dE_{gap}/d\sigma|$ of typical bulk semiconductors. Note that half of all semiconducting NTs ($p = 1$) will have $dE_{gap}/d\sigma > 0$, while the other half ($p = -1$) have $dE_{gap}/d\sigma < 0$.

With knowledge of this electromechanical effect, we first interpret the constant-tip-voltage experiments. When

strain causes G to decrease (increase), $dE_{gap}/d\sigma$ is positive (negative). If G does not change, then $dE_{gap}/d\sigma$ is close enough to zero to be undetectable.

The G-V_{tip} curves shown in Fig. 4 confirm this picture. We assume that the tip gate affects the middle portion of the tube while sections close to the contacts are held p-type [30]. Sweeping V_{tip} will change the strained tube from a p-doped semiconductor [$V_{tip} = 0$, Fig. 5(a)] to a p-n-p junction [$V_{tip} > 1$ V, Fig. 5(c)]. The conductance minimum at ~ 1 V corresponds to charge carrier depletion in the NT's middle section during the transition from p-type to n-type [Fig. 5(b)]; the size of the conductance dip depends on the band gap E_{gap}, which changes with strain.

To model the resistance $R_{max}(\sigma)$ associated with this conductance minimum, we consider transport by thermal activation, neglecting tunneling across the depleted region. Referring to Fig. 5(b), electrons with energy E such that $|E - E_F| > E_{gap}$ cross the barrier with a transmission probability $|t|^2$, while those with $|E - E_F| < E_{gap}$ are reflected. The low-bias resistance of the device is then

$$R_{tot} = R_S + \frac{1}{|t|^2}\frac{h}{8e^2}\left[1 + \exp\left(\frac{E_{gap}}{kT}\right)\right], \qquad (4)$$

where the first term R_S is the resistance in series with the junction due to the metal-NT contacts, etc., and the second term is the resistance of the junction region. From Eq. (3), we have

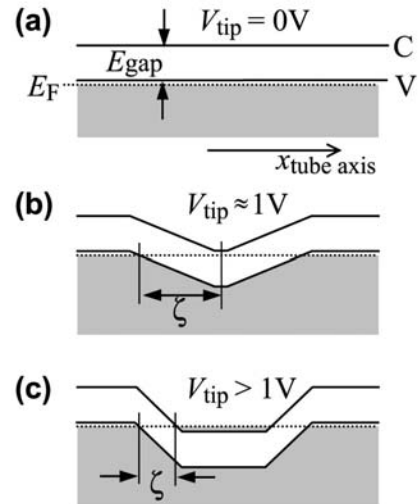$$E_{gap} = E_{gap}^0 + \frac{dE_{gap}}{d\sigma}\sigma. \qquad (5)$$

FIG. 5. Evolution of the energy band diagram as V_{tip} is increased. The tube is held p-type at the contacts. The valence and conduction band edges are denoted by V and C. (a) $V_{tip} = 0$ V, the NT is a p-type semiconductor. (b) $V_{tip} \approx 1$ V, transport is interrupted by a depleted region. (c) $V_{tip} > 1$ V, a p-n-p junction forms in the middle of the tube. Transport due to tunneling increases as the distance ζ becomes smaller.

156401-3

156401-3

Equations (4) and (5) give physical meaning to the fitting parameters β, R_0, and R_1 that were introduced in Eq. (2). Most important is β, the exponential fitting parameter, which is related to the strain dependence of the gap: $dE_{gap}/d\sigma = \beta kT$. From the measured values of β, we obtain $dE_{gap}/d\sigma = -53$ meV/% for the semiconducting tube in Fig. 4(b) and $dE_{gap}/d\sigma = +35$ meV/% for the metallic tube in Fig. 4(a). From Eq. (3), we can then estimate chiral angles $\phi \approx 19°$ and $23°$ for the two tubes, respectively. For an accurate determination of the chiral angles, additional experiments are necessary to verify the quantitative validity of Eqs. (3) and (4).

Additional knowledge about the device can be gained from the fitting parameter $R_1 = (h/8e^2|t|^2)\exp(E_{gap}^0/kT)$. Fitting results for the metallic tube ($E_{gap}^0 = 0$) gives $R_1 = 0.49h/e^2$, and, hence, a transmission probability $|t|^2 = 0.25$. Transport of thermally activated electrons across the junction region is thus not ballistic, but nevertheless highly transmissive, as expected from previous measurements of long mean-free paths in NTs [31]. Fitting the semiconducting tube data yields a much higher resistance, $R_1 = 171h/e^2$. Using an estimate of $|t|^2 = 0.25$ from above, we infer $E_{gap}^0 = 160$ meV. This inferred energy gap corresponds to a tube with diameter $d = 4.7$ nm (using $E_{gap} = 2t_0r_0/d$ [32]), in reasonable agreement with $d = 4 \pm 0.5$ nm measured by AFM. The agreement provides support for the validity of Eq. (4). However, variable temperature studies are needed to definitively separate out the tunneling and thermal activation contributions [33]; unfortunately, this is not possible with our current AFM.

The use of strain to continuously tune the band gap of a NT has a number of potential applications. Accurate measurements of $dE_{gap}/d\sigma$ may be used to uniquely determine the wrapping indices of small-diameter tubes. Electrical transduction of small forces is also possible; for example, the most sensitive device studied here has a sensitivity of 0.1 nN/Hz$^{1/2}$ at low frequencies. Finally, NT heterostructures, where different sections of a single NT have different band gaps, can be created if the different sections can be selectively strained.

---

[1] T. W. Odom et al., Nature (London) **391**, 62 (1998).

[2] J. W. G. Wildoer et al., Nature (London) **391**, 59 (1998).

[3] M. F. Yu et al., Science **287**, 637 (2000).

[4] J. P. Salvetat et al., Appl. Phys. A **69**, 255 (1999).

[5] R. Heyd, A. Charlier, and E. McRae, Phys. Rev. B **55**, 6820 (1997).

[6] C. L. Kane and E. J. Mele, Phys. Rev. Lett. **78**, 1932 (1997).

[7] A. Rochefort, D. R. Salahub, and P. Avouris, Chem. Phys. Lett. **297**, 45 (1998).

[8] L. Yang et al., Phys. Rev. B **60**, 13 874 (1999).

[9] S. Paulson , et al., Appl. Phys. Lett. **75**, 2936 (1999).

[10] T. W. Tombler et al., Nature (London) **405**, 769 (2000).

[11] L. Yang and J. Han, Phys. Rev. Lett. **85**, 154 (2000).

[12] A. Maiti, A. Svizhenko, and M. P. Anantram, Phys. Rev. Lett. **88**, 126805 (2002).

[13] J. Lee et al., Nature (London) **415**, 1005 (2002).

[14] D. A. Walters et al., Appl. Phys. Lett. **74**, 3803 (1999).

[15] J. P. Salvetat et al., Phys. Rev. Lett. **82**, 944 (1999).

[16] J. Nygard and D. H. Cobden, Appl. Phys. Lett. **79**, 4216 (2001).

[17] N. R. Franklin et al., Appl. Phys. Lett. **81**, 913 (2002).

[18] J. Kong et al., Nature (London) **395**, 878 (1998).

[19] S. Rosenblatt et al., Nano Lett. **2**, 869 (2002).

[20] Many of the etched devices are not robust, as evidenced by degradation of electrical contact during AFM imaging. The data presented here is from NTs that have robust contact with the gold electrodes.

[21] J. Y. Park et al., Appl. Phys. Lett. **80**, 4446 (2002).

[22] J. L. Hutter and J. Bechhoefer, Rev. Sci. Instrum. **64**, 1868 (1993).

[23] For consistent NT-tip alignment, the x-y piezo must be stabilized for many minutes. As a NT is pushed, tip deflection can jump suddenly toward zero. Slack is not changed by these events; therefore we associate such jumps with slips of the NT-tip contact. Favorable contact is achieved by trial and error. A low noise laser, available by special request from Digital Instruments technical support, suppresses laser interference effects that can contaminate tip deflection data.

[24] B. I. Yakobson, C. J. Brabec, and J. Bernholc, Phys. Rev. Lett. **76**, 2511 (1996).

[25] X. Zhou, J. J. Zhou, and Z. C. Ou-Yang, Phys. Rev. B **62**, 13 692 (2000).

[26] J. P. Lu, Phys. Rev. Lett. **79**, 1297 (1997).

[27] S. Decossas et al., Europhys. Lett. **53**, 742 (2001).

[28] Uncertainty in YA comes from uncertainty in L_0, x-y tip positioning, and the cantilever spring constant.

[29] The PtIr metal coating on the AFM tip makes very poor electrical contact with the NT with typical leakage resistance $> 10\,\mathrm{G\,\Omega}$.

[30] J. W. Park and P. L. McEuen, Appl. Phys. Lett. **79**, 1363 (2001).

[31] A. Bachtold et al., Phys. Rev. Lett. **84**, 6082 (2000).

[32] C. T. White and J. W. Mintmire, Nature (London) **394**, 29 (1998).

[33] We have investigated the assumption that electron tunneling does not contribute significantly to R_{max} [Eq. (4), Fig. 5(b)] by calculating the tunneling resistance for different junction electric fields $\varepsilon = E_{gap}/\zeta$. For $\varepsilon < 10^7$ V/m (corresponding to $\zeta > 20$ nm when $E_{gap} = 200$ meV), the effect of tunneling is negligible. Similar calculations and estimates of ζ are found in F. Leonard and J. Tersoff, Phys. Rev. Lett. **83**, 5174 (1999); A. A. Odintsov, Phys. Rev. Lett. **85**, 150 (2000).